Journal of Engineering Mechanics and Machinery (2024)
Clausius Scientific Press, Canada
DOI: 10.23977/jemm.2024.090215
ISSN 2371-9133 Vol. 9 Num. 2

Finite Element Analysis of Rotor Strength in High-Speed Permanent Magnet Generators

Dongni Zhang*

CRRC Zhuzhou Electric Co., Ltd., Zhuzhou, Hunan, 412001, China
011600080473@crrcgc.cc
*Corresponding author

Keywords: High-speed permanent magnet, generator, rotor, strength, finite element

Abstract: This study systematically analyzes the stress distribution of the rotor in high-speed permanent magnet generators under different conditions, including rotor structure, types of inter-pole filler materials, sleeve thickness, interference fit, temperature, and rotational speed, using finite element analysis (FEA). The results indicate that circumferential segmentation can significantly reduce the tangential and radial stresses of the permanent magnets, with the best performance observed in the rotor structure with four segments. However, increasing the number of segments (e.g., to 20 segments) does not significantly improve the stress distribution in the sleeve and core, and in some cases, it may even exacerbate stress concentration. Regarding the choice of inter-pole filler materials, high-temperature-resistant plastic (PPS) performs best in reducing the stress on both the permanent magnets and the sleeve. Compared to carbon fiber and aluminum alloy materials, PPS more effectively reduces the stress on the permanent magnets and sleeve, especially under high-temperature and high-speed conditions, showing superior mechanical performance. Increasing the sleeve thickness effectively reduces both the tangential and radial stresses of the permanent magnets, while also decreasing the equivalent stress in the sleeve, thus enhancing the structural safety of the rotor. As the interference fit increases, the radial stress on the permanent magnets gradually decreases, while the tangential and equivalent stresses in the sleeve first increase slowly and then rapidly. When the interference fit is below 0.26 mm, the stress variation is minimal, but once it exceeds 0.26 mm, the sleeve stress increases significantly, indicating that excessive interference may lead to stress concentration and a higher risk of failure. Temperature elevation significantly increases the tangential and equivalent stresses in the permanent magnets, and the tangential and equivalent stresses in the sleeve also increase linearly with rising temperatures. At high rotational speeds, the maximum tangential stress experienced by both the permanent magnets and the sleeve increases substantially, highlighting the need for careful optimization of materials and structure in the design phase.

1. Introduction

Designing high-speed permanent magnet generators presents several challenges[1]. Due to the small size and high rotational speed of the rotors in such generators, overheating of the rotor can easily occur. This overheating not only affects the stress distribution across various parts of the rotor[2] but also leads to irreversible demagnetization of the permanent magnets. The combined issues of heating and mechanical strength of the rotor limit the maximum power output and rotational speed of large high-speed motors[3]. Therefore, studying the rotor strength of high-speed permanent magnet synchronous generators is of great significance, as it can provide useful insights for the comprehensive design of high-power, high-speed permanent magnet motors.

Shen et al.[4] proposed a minimum thickness design method for the rotor sleeve of permanent magnet motors, developing a two-dimensional stress field analytical model. They validated this model using finite element analysis (FEA). Wang et al.[5] employed the FEA method to analyze the stresses in the rotor of a high-speed permanent magnet motor with segmented magnets retained by carbon-fiber sleeves and proposed a corresponding sleeve thickness design. Lee and Hong[6] combined theoretical and finite element analyses to compare the mechanical properties of metal-sleeved and composite-sleeved rotors. Du et al.[7] conducted a detailed stress analysis of the rotor using FEA, considering various multi-physics constraints and their impacts. Zhang et al.[8] used a combination of optimization methods and FEA to optimize the geometric dimensions of the rotor, effectively reducing its mass. Du et al.[9] performed a comparative FEA study on six different rotor structures and sleeve materials, selecting the optimal rotor design. Yang Jiangtao et al.[10] developed a theoretical analytical model to calculate rotor stress considering interference fits and validated the analytical solutions with FEA. Zhou et al.[11] explored the use of carbon fiber-reinforced plastic as a rotor sleeve material, using various analytical methods to evaluate the performance of the carbon fiber-reinforced sleeve.

This study uses the finite element method[12-14] to analyze the strength of the rotor in high-speed permanent magnet synchronous motors. It focuses on selecting the appropriate interference fit, sleeve materials, and inter-pole filler materials. The study also examines the effects of different rotor structures on the stress experienced by various rotor components, as well as the impact of sleeve thickness, temperature, and rotational speed, providing valuable references for the design of high-speed permanent magnet synchronous motor rotors in practical applications [15].

2. Analysis of the Impact of Rotor Structure Types on Rotor Strength

2.1 Introduction to Rotor Structure Types

Four different rotor structures, as shown in Figure 1, were analyzed in this study. Figure 1(a) corresponds to a rotor structure where the permanent magnets are not segmented circumferentially. Figure 1(b) shows a structure where the permanent magnets are divided into four circumferential segments. Figure 1(c) presents a structure with 20 circumferential segments, and Figure 1(d) depicts a rotor structure that uses an inner-pole eccentric chamfering technique.

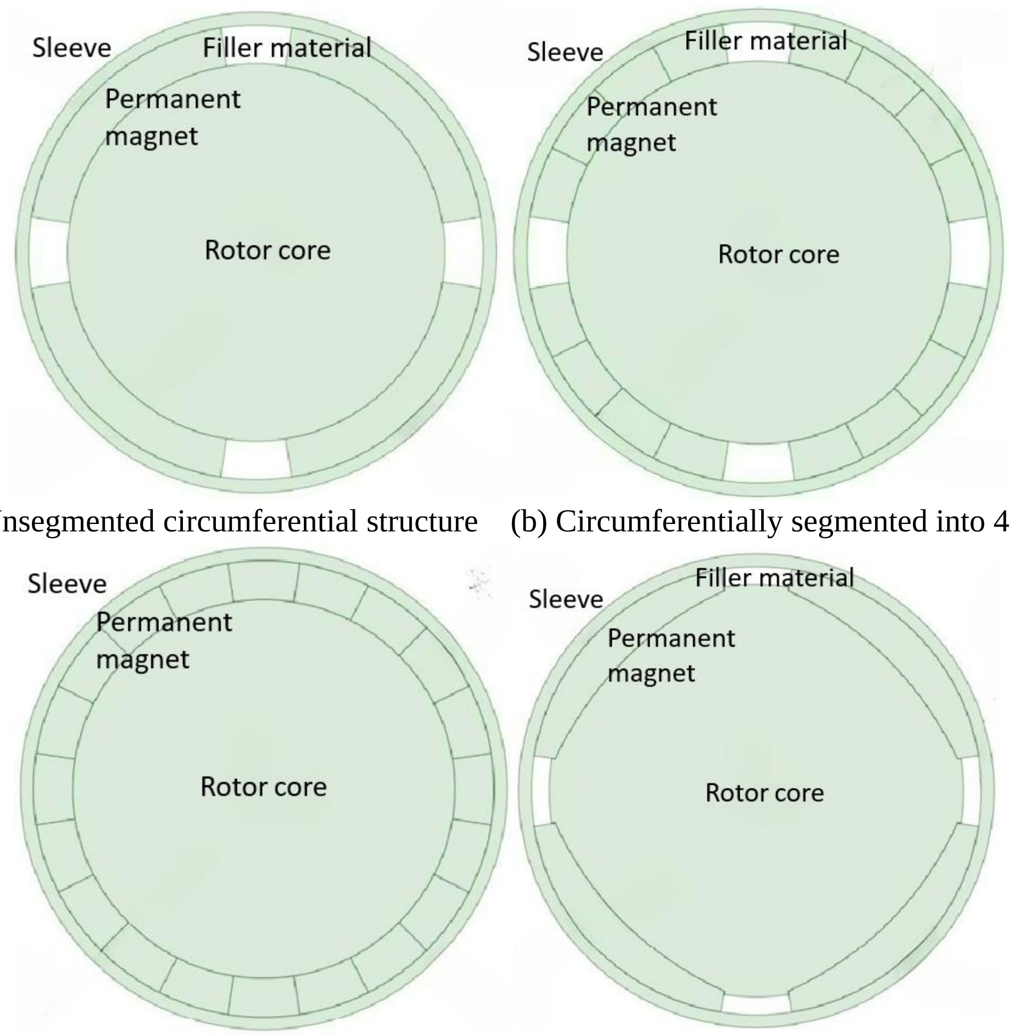

(a) Unsegmented circumferential structure (b) Circumferentially segmented into 4 parts

(c) Circumferentially segmented into 20 parts (d) Inner-pole eccentric chamfering technique

Figure 1: Four Types of Rotor Structures

2.2 Analysis of the Impact of Rotor Structure Types on Strength

The finite element simulation used model dimensions based on actual engineering parameters. The operating temperature was set at 120 ℃, and the rotational speed was set to 1.2 times the rated speed, i.e., 21,600 rpm. For each of the four rotor structures, the tangential and radial stresses in the permanent magnets, the equivalent stress in the sleeve, and the equivalent stress in the rotor core were calculated. The stresses experienced by each component of the four rotor structures are shown in Table 1.

As shown in Table 1, the comparison of the maximum tangential stress of the permanent magnets shows that circumferential segmentation effectively reduces the tangential stress of the permanent magnets, especially in the case of the four-segment structure, where the stress is reduced by approximately 50.6%. However, as the number of segments increases to 20, the tangential stress rises slightly but remains significantly lower than that of the unsegmented structure. The inner-pole eccentric chamfering treatment, however, leads to a substantial increase in tangential stress, likely due to stress concentration caused by this treatment method. As Table 1 shows, the comparison of the maximum radial stress of the permanent magnets demonstrates that increasing the number of segments effectively reduces the radial stress of the permanent magnets. Specifically, the 20-segment structure reduces the radial stress by 29.4% compared to the unsegmented structure. However, the inner-pole eccentric chamfering treatment leads to a notable increase in radial stress.

Table 1: Comparison of Calculated Stresses for Different Rotor Structure Types

Rotor Structure Type	Maximum Tangential Stress in Permanent Magnets (MPa)	Maximum Radial Stress in Permanent Magnets (MPa)	Maximum Equivalent Stress in Rotor Core (MPa)	Maximum Equivalent Stress in Sleeve (MPa)
Unsegmented Circumferential Structure	92.5631	51.4178	132.8617	321.0732
Circumferentially Segmented into 4 Parts	45.7120	44.1238	79.0534	315.1342
Circumferentially Segmented into 20 Parts	54.3015	36.3063	128.9704	318.1983
Inner-Pole Eccentric Chamfering Technique	136.5204	56.8867	215.6673	311.5214

As shown in Table 1, the comparison of maximum equivalent stress in rotor core highlights that circumferential segmentation is also effective in reducing the equivalent stress of the rotor core, particularly in the four-segment structure, where the stress is reduced by approximately 40.5%. However, when the number of segments increases to 20, the rotor core’s stress returns to levels similar to that of the unsegmented structure. The inner-pole eccentric chamfering treatment causes a significant increase in the rotor core’s stress, indicating that this method does not effectively improve the rotor core’s stress distribution. The comparison of the maximum equivalent stress in the sleeve suggests that circumferential segmentation has a minimal effect on the sleeve stress, reducing it by less than 2%. The inner-pole eccentric chamfering treatment also has a negligible impact on the sleeve stress, which remains relatively stable.

From a qualitative perspective, both circumferential segmentation and inner-pole eccentric chamfering treatment have distinct characteristics. In the four-segment configuration, stress in all components is effectively reduced, indicating that this segmentation method alleviates stress concentration. However, when the number of segments increases to 20, although the radial and tangential stresses in the permanent magnets decrease further, the stress in the sleeve and rotor core does not show a significant reduction and, in some cases, even increases. This may be due to the structural complexity and localized stress concentration caused by excessive segmentation. The inner-pole eccentric chamfering treatment significantly increases both radial and tangential stresses in the permanent magnets and also leads to a substantial rise in the rotor core stress. This indicates that while the chamfering technique may improve certain characteristics, it may worsen stress distribution, resulting in higher loads on the rotor core. Although the sleeve stress is not significantly affected, stress concentration in the permanent magnets may negatively impact long-term operation.

3. Analysis of the Impact of Inter-Pole Filler Materials on Rotor Strength

The tile-shaped permanent magnets are separated by filler materials, which serve to fix and protect the magnets. According to the previous finite element analysis (FEA) results, the maximum radial stress in the permanent magnets and the maximum equivalent stress in the sleeve often occur at the points where the filler material contacts the magnets. For surface-mounted high-speed permanent magnet motors, selecting the appropriate inter-pole filler material can reduce the maximum equivalent stress in the sleeve and the maximum radial stress in the permanent magnets. Therefore, analyzing the effects of different filler materials on the stresses in the permanent magnets and the sleeve provides a theoretical foundation for choosing suitable filler materials. Common inter-pole filler materials include high-temperature-resistant plastic (PPS), carbon fiber, and alloy materials. From the previous analysis, it is evident that the rotor structure with four circumferential segments exhibits the best stress performance. Therefore, this structure was selected for finite element analysis of the impact of different inter-pole filler materials on rotor strength. The operating temperature was set to 120 ℃, and the rotational speed was set to 1.2 times the rated speed. The maximum stresses in various parts of the rotor for the three different filler materials are shown in Table 2.

As shown in Table 2, the aluminum alloy has the highest tangential stress, exceeding that of PPS by 2.1877 MPa (approximately 4.5%) and exceeding that of carbon fiber by 1.3031 MPa (approximately 2.7%). This indicates that, in terms of tangential stress in the permanent magnets, high-temperature-resistant plastic PPS performs the best. As shown in Table 2, carbon fiber has the highest maximum radial stress, reaching 51.3121 MPa, which is 0.8757 MPa (approximately 1.7%) higher than that of aluminum alloy and 3.034 MPa (approximately 6.3%) higher than that of PPS. Therefore, in terms of radial stress in the permanent magnets, high-temperature-resistant plastic PPS clearly outperforms the other two materials. As shown in Table 2, in terms of equivalent stress in the sleeve, aluminum alloy has the highest value of 329.3367 MPa, which is 12.3535 MPa (approximately 3.9%) higher than that of PPS and 16.8769 MPa (approximately 5.4%) higher than that of carbon fiber. Relatively speaking, carbon fiber performs slightly better than the other two materials in terms of sleeve equivalent stress. In summary, PPS plastic is the most suitable choice as the filler material.

Table 2: Comparison of Stresses in a Rotor Structure Segmented into 4 Parts with Different Inter-Pole Filler Materials

Type of Inter-Pole Filler Material	Maximum Tangential Stress in Permanent Magnets (MPa)	Maximum Radial Stress in Permanent Magnets (MPa)	Maximum Equivalent Stress in Sleeve (MPa)
High-Temperature Plastic (PPS)	48.1321	48.2781	316.9832
Aluminum Alloy	50.3198	50.4364	329.3367
Carbon Fiber	49.0167	51.3121	312.4598

When using the permanent magnet structure treated with inner-pole eccentric chamfering, as shown in Figure 1(d), an analysis of the stresses experienced by the rotor with different filler materials was conducted. The filler materials could include the commonly used materials mentioned above or materials consistent with the rotor yoke material, forming an integrated structure known as a surface-inserted rotor. The stresses experienced by the rotor when using PPS plastic and carbon steel as filler materials are shown in Table 3.

As shown in Table 3, the maximum tangential stress in the permanent magnets using high-temperature-resistant plastic (PPS) is 136.5204 MPa, while for the integrated structure, the maximum tangential stress is 147.2631 MPa, which is 10.7426 MPa higher than that of PPS, representing an increase of approximately 7.87%. Regarding the maximum radial stress in the permanent magnets, PPS shows a value of 56.8867 MPa, while the integrated structure shows a value of 25.7543 MPa. Comparatively, the integrated structure reduces the maximum radial stress by 31.1324 MPa, a decrease of 54.72%. This reduction is likely due to the deeper dovetail groove in the rotor core, which helps secure the permanent magnets and lowers the radial stress. For the maximum equivalent stress in the rotor core, PPS exhibits a value of 215.6673 MPa, whereas the integrated structure shows 140.6832 MPa. The equivalent stress in the rotor core using PPS is 74.9841 MPa higher, representing an increase of 53.3%. Therefore, in terms of equivalent stress in the rotor core, the integrated structure performs better. Regarding the maximum equivalent stress in the sleeve, PPS shows a value of 311.5214 MPa, while the integrated structure exhibits 317.2908 MPa. The difference between these values is minimal. From the above analysis, it can be concluded that the surface-inserted rotor with an integrated structure has clear stress advantages.

Table 3: Comparison of Stresses in Rotor Structure with Inner-Pole Eccentric Chamfering under Different Inter-Pole Filler Materials

Type of Inter-Pole Filler Material	Maximum Tangential Stress in Permanent Magnets (MPa)	Maximum Radial Stress in Permanent Magnets (MPa)	Maximum Equivalent Stress in Rotor Core (MPa)	Maximum Equivalent Stress in Sleeve (MPa)
High-Temperature Plastic (PPS)	136.5204	56.8867	215.6673	311.5214
Carbon Steel (Integrated Structure)	147.2631	25.7543	140.6832	317.2908
Further Segmentation	61.3971	64.4138	125.9632	323.0746

The results in Table 1 demonstrate that circumferential segmentation can significantly improve the stress performance of the rotor structure. By further applying circumferential segmentation to the surface-inserted rotor structure, the stress distribution is further optimized. The four permanent magnets in Figure 1(d) were each subdivided into four smaller segments. After segmentation, the stress on the rotor was recalculated as shown in Table 3. The maximum tangential stress in the permanent magnets decreased significantly from 147.2631 MPa to 61.3971 MPa, indicating a substantial reduction in tangential stress. However, the maximum radial stress increased from 25.7543 MPa to 64.4138 MPa. The equivalent stresses in the rotor core and sleeve showed minimal change after segmentation.

4. Analysis of Factors Affecting Rotor Strength

4.1 The Impact of Sleeve Thickness on Rotor Stress

The selection of sleeve thickness must take into account factors such as electromagnetic performance, heat dissipation, and stress distribution. If the sleeve is too thick, it can hinder the heat dissipation of the permanent magnets and reduce the effective air gap length, increasing the risk of rotor-to-stator rubbing. On the other hand, if the sleeve is too thin, the stress on the permanent magnets increases, reducing their protection. Using the rotor structure with four circumferential segments as shown in Figure 1(b), the stress distribution in various parts of the rotor was analyzed for different sleeve thicknesses. The results are shown in Figure 2 (a).

As shown in Figure 2 (a), as the sleeve thickness increases, the maximum tangential stress in the permanent magnets decreases from approximately 57 MPa to about 49 MPa, indicating that increasing the sleeve thickness effectively reduces the tangential stress experienced by the permanent magnets. Similarly, the maximum radial stress in the permanent magnets follows a similar trend, decreasing from approximately 47 MPa to about 45 MPa. The maximum equivalent stress in the sleeve decreases from around 333 MPa to approximately 305 MPa, suggesting that a thicker sleeve also helps reduce the maximum equivalent stress experienced by the sleeve. The average equivalent stress in the sleeve follows a similar downward trend, dropping from about 310 MPa to approximately 285 MPa. From this quantitative analysis, it is clear that increasing the sleeve thickness not only reduces the tangential stress in the permanent magnets but also decreases both the maximum and average equivalent stress in the sleeve, positively impacting the structural safety and lifespan of the generator.

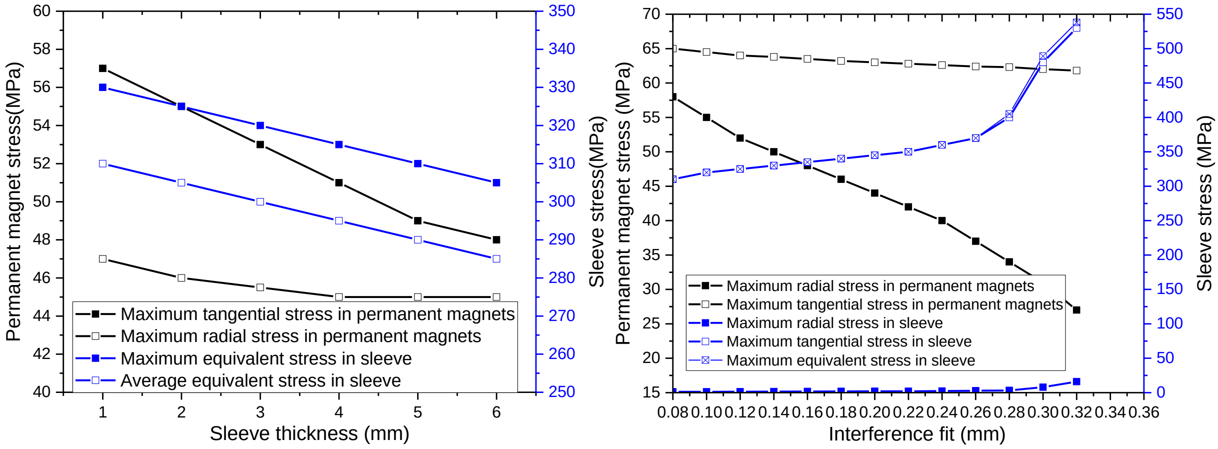

(a) Calculated Rotor Stresses at Different Sleeve Thicknesses (Left)
(b) Calculated Rotor Stresses at Different Interference Fits (Right)

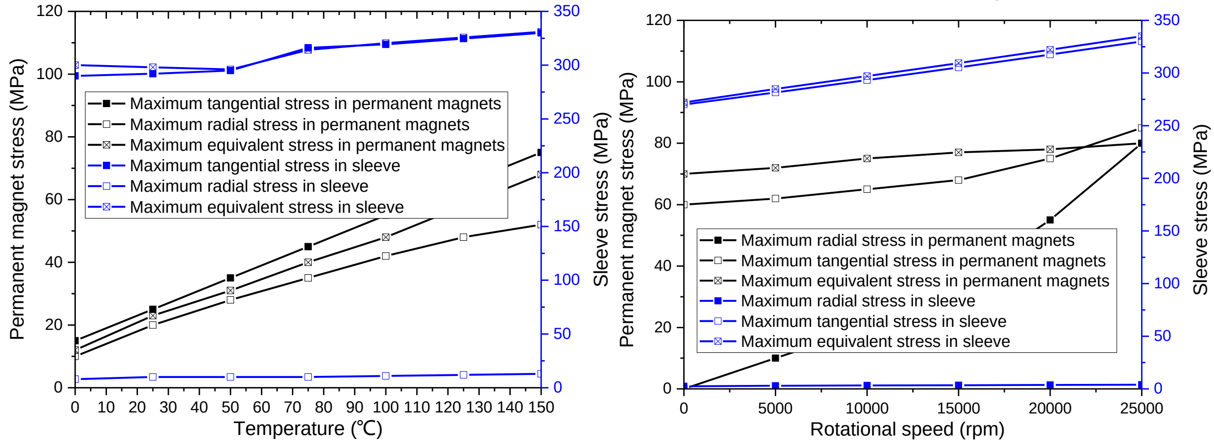

(c) Calculated Rotor Stresses at Different Temperatures (Left)
(d) Calculated Rotor Stresses at Different Rotational Speeds (Right)

Figure 2: The corresponding calculation results of each influencing factor

4.2 The Impact of Interference Fit on Rotor Stress

Using the rotor structure with four circumferential segments, as shown in Figure 1(b), the stress changes in various parts of the rotor were analyzed under different interference fits. The interference fits were set between 0.08 mm and 0.32 mm, with stress calculations conducted at 0.02 mm increments to observe the effects of interference fit on the stresses experienced by the permanent magnets and sleeve. The results are shown in Figure 2 (b). As the interference fit increases, the maximum radial stress in the permanent magnets shows a gradual downward trend, decreasing from an initial value of nearly 58 MPa to approximately 26 MPa. This entire process demonstrates a clear reduction in stress. Similarly, the tangential stress in the permanent magnets also shows a slight, gradual reduction as the interference fit increases. The tangential stress in the sleeve, however, exhibits a different pattern. Initially, it increases slowly as the interference fit increases, but once the interference fit exceeds approximately 0.26 mm, the tangential stress begins to rise rapidly. The maximum equivalent stress in the sleeve follows the same trend as the tangential stress, with both experiencing slow increases at first, followed by a rapid rise once the interference fit reaches 0.26 mm. During the initial phase, the stress variation is minimal, but after the interference fit exceeds 0.26 mm, the stresses increase significantly. This analysis shows that increasing the interference fit has a notable impact on the stress distribution in the rotor. While it reduces the radial stress in the permanent magnets, it simultaneously increases the stress in the sleeve, particularly when the interference fit exceeds 0.26 mm.

In practical generator rotor design, it is essential to adjust design parameters based on the actual interference fit to ensure that the stress distribution in the permanent magnets and sleeve remains within a safe range. This helps to prevent material failure or fatigue damage caused by excessive stress. When selecting the appropriate interference fit, it is crucial to balance the reduction in radial stress with the increase in tangential and equivalent stresses in the sleeve, aiming to find an optimal balance point that ensures the reliability and performance of the overall structure.

4.3 The Impact of Temperature on Rotor Stress

Taking the unsegmented rotor structure shown in Figure 1(a) as an example, the impact of temperature on the stresses experienced by various parts of the rotor is analyzed. The initial temperature of the rotor is set to 22 ℃, and the operating temperature ranges from 0 ℃ to 150 ℃, while the rotational speed is set to 1.2 times the rated speed. The trends of key stresses in the permanent magnets and the sleeve as a function of temperature are shown in Figure 2 (c).

As shown in Figure 2 (c)., the maximum tangential stress, maximum radial stress, and maximum equivalent stress in the permanent magnets exhibit a rapid linear increase as the temperature rises. Similarly, the maximum tangential and equivalent stresses in the sleeve also increase almost linearly with temperature, but at a slower rate compared to the stresses in the permanent magnets. The maximum radial stress in the sleeve is minimally affected by temperature changes.It can be inferred that the stress values in the permanent magnets are more sensitive to temperature variations, which is closely related to factors such as the material's thermal expansion coefficient and mechanical properties. The increase in temperature leads to a continuous rise in stress values in both the permanent magnets and the sleeve, with the stress in the permanent magnets increasing more significantly. Therefore, the design of generator rotors must fully consider the impact of temperature on material stresses to ensure that the structural integrity and mechanical stability of the materials are maintained under high-temperature conditions.

4.4 The Impact of Rotational Speed on Rotor Stress

Similarly, using the unsegmented rotor structure shown in Figure 1(a) as an example, the working environment temperature is set to 120 ℃, and only the rotational speed of the rotor is varied. The rotor speed is gradually increased from 0 to 25,000 rpm, with six key points selected for analysis. At these six points, the radial stress, tangential stress, and equivalent stress in the permanent magnets and sleeve are calculated. The effect of rotational speed on the stresses experienced by the permanent magnets and sleeve is shown in Figure 2 (d).

As shown in Figure 2 (d), the maximum radial stress in the permanent magnets increases steadily with rising rotational speed. As the speed increases from 0 to 25,000 rpm, the radial stress in the permanent magnets rises from approximately 0 MPa to around 80 MPa. This indicates a clear linear relationship, with radial stress in the permanent magnets gradually increasing as the rotational speed increases. The maximum tangential stress in the permanent magnets also rises with increasing speed. Starting at a relatively low stress level of around 60 MPa, the stress increases gradually to about 85 MPa when the speed reaches 25,000 rpm. Similarly, the maximum equivalent stress in the permanent magnets increases with speed, starting from 70 MPa and reaching approximately 80 MPa at 25,000 rpm. The stresses in the sleeve follow a similar trend as rotational speed increases. While the maximum radial stress in the sleeve shows little change as the speed increases from 0 to 25,000 rpm, the maximum tangential stress and equivalent stress increase significantly, rising from around 280 MPa to 330 MPa. This indicates that the sleeve experiences significant stress, particularly in terms of tangential and equivalent stresses, as the rotor operates at higher speeds.

Overall, with the increase in rotational speed, the stress experienced by both the permanent magnets and the sleeve material shows a significant upward trend. The radial stress in the permanent magnets exhibits the largest increase, followed by the maximum tangential stress in the permanent magnets, the maximum tangential stress in the sleeve, and the maximum equivalent stress in the sleeve. The smallest increases are seen in the maximum equivalent stress in the permanent magnets and the maximum radial stress in the sleeve. The increase in speed leads to an enhanced centrifugal force, causing the permanent magnets and sleeve material to endure greater tensile and compressive stresses at high rotational speeds. Therefore, when designing generators, careful consideration must be given to material selection and structural optimization to ensure safe operation under high-speed conditions.

5. Conclusion

This study systematically analyzed the stress distribution in the rotor of a high-speed permanent magnet generator under different conditions, including rotor structure, types of inter-pole filler materials, sleeve thickness, interference fit, temperature, and rotational speed, using the finite element analysis method. The key conclusions are as follows:

(1) Circumferential segmentation significantly reduces both the tangential and radial stresses in the permanent magnets, with the rotor structure segmented into four parts showing the best performance. However, increasing the number of segments (e.g., to 20) does not lead to significant improvements in the stresses on the sleeve and core, and in some cases, it may even cause stress concentration.

(2) In terms of inter-pole filler material selection, high-temperature-resistant plastic PPS performs best in reducing stresses in both the permanent magnets and the sleeve. Compared to carbon fiber and aluminum alloy materials, PPS is more effective in lowering these stresses, especially under high-temperature and high-speed conditions, where it exhibits superior mechanical performance.

(3) Increasing the sleeve thickness effectively reduces both the tangential and radial stresses in the permanent magnets while also decreasing the equivalent stress in the sleeve. A thicker sleeve enhances the structural safety of the rotor. As the interference fit increases, the radial stress in the permanent magnets gradually decreases, while the tangential and equivalent stresses in the sleeve first increase slowly and then rapidly. When the interference fit is less than 0.26 mm, stress changes are minimal; however, when it exceeds 0.26 mm, the sleeve stress increases significantly, indicating that excessive interference may lead to stress concentration and a higher risk of failure. An increase in temperature significantly raises the tangential and equivalent stresses in the permanent magnets, with

the sleeve's tangential and equivalent stresses also increasing linearly with temperature. Under high rotational speeds, the tangential stresses in both the permanent magnets and the sleeve increase significantly, necessitating careful optimization of material selection and structural design to ensure safe operation.

References

[1] Gallicchio, G., Di Nardo, M., Palmieri, M., Ilkhani, M. R., Degano, M., Gerada, C., & Cupertino, F. (2022). Surface permanent magnet synchronous machines: High speed design and limits. IEEE Transactions on Energy Conversion, 38(2), 1311-1324.

[2] Hou, P., Ge, B., Tao, D., Pan, B., & Wang, Y. (2022). Rotor strength analysis of feco-based permanent magnet high speed motor. Machines, 10(6), 462.

[3] Wang, L., Du, G., Tong, J., Huang, N., Hu, C., & Xu, W. (2021, December). Comparation of different rotor sleeves of highspeed permanent magnet synchronous motors based on multi-physics. In 2021 IEEE 4th Student Conference on Electric Machines and Systems (SCEMS) (pp. 1-5). IEEE.

[4] Shen Jianxin, Qin Xuefei, Yao Lei, & Wang Yunchong. (2022). Strength Analysis and Sleeve Design of High-Speed Permanent Magnet Motor Rotors. Proceedings of the Chinese Society for Electrical Engineering, 42(6), 2334-2345.

[5] Wang, Y., Zhu, Z. Q., Feng, J., Guo, S., & Li, Y. (2020). Rotor stress analysis of high-speed permanent magnet machines with segmented magnets retained by carbon-fibre sleeve. IEEE Transactions on Energy Conversion, 36(2), 971-983.

[6] Lee, T. W., & Hong, D. K. (2022). Rotor design, analysis and experimental validation of a high-speed permanent magnet synchronous motor for electric turbocharger. IEEE Access, 10, 21955-21969.

[7] Du, G., Huang, N., He, H., Lei, G., & Zhu, J. (2020). Parameter design for a high-speed permanent magnet machine under multiphysics constraints. IEEE Transactions on energy conversion, 35(4), 2025-2035.

[8] Zhang, Y., Tang, J., & Xu, X. (2022). Modal analysis and multidisciplinary optimization of disk-shaped rotor in MSCMG. International Journal of Mechanical Sciences, 226, 107387.

[9] Du, G., Pu, T., Zhou, Q., Wang, L., Lei, G., & Zhu, J. (2023). Multiphysics comparative study of high speed PM machines for ring PM rotor and solid PM rotor. IEEE Transactions on Energy Conversion, 38(2), 1421-1432.

[10] Yang Jiangtao, Wang Zhenyu, Feng Yaojing, & Huang Shoudao. (2023). The Impact of Interference Fit on Rotor Stress in High-Speed Permanent Magnet Motors. Transactions of China Electrotechnical Society, 38(16), 4263-4273.

[11] Zhou, Y., Tian, L., Gao, S. H., Zhang, J. W., Yang, L. K., & Xie, R. G. (2021). Design and testing of CFRP sleeve for a high-speed permanent magnet synchronous motor with surface-mounted rotor. Journal of Mechanical Science and Technology, 35(1), 221-230.

[12] Meng X, Geng D, Liu S. The modified Mohr-Coulomb model considering softening effect and intermediate principal stress [J]. Mechanics of Advanced Materials and Structures, 2024: 1-15.

[13] Yan S, Geng D, Dai N, et al. An improved dual shear unified strength model (IDSUSM) considering strain softening effect [J]. International Journal of Damage Mechanics, 2024.

[14] Geng D, Dai N, Guo P, et al. Implicit numerical integration of highly nonlinear plasticity models[J]. Computers and Geotechnics, 2021, 132: 103961.

[15] Chen H, Yang Y, & Shao C. Multi-task learning for data-efficient spatiotemporal modeling of tool surface progression in ultrasonic metal welding. Journal of Manufacturing Systems, 2021, 58, 306-315.